

SCIENTIFIC REPORTS



OPEN

Predicted reentrant melting of dense hydrogen at ultra-high pressures

Hua Y. Geng & Q. Wu

Received: 06 June 2016
 Accepted: 20 October 2016
 Published: 11 November 2016

The phase diagram of hydrogen is one of the most important challenges in high-pressure physics and astrophysics. Especially, the melting of dense hydrogen is complicated by dimer dissociation, metallization and nuclear quantum effect of protons, which together lead to a *cold melting* of dense hydrogen when above 500 GPa. Nonetheless, the variation of the melting curve at higher pressures is virtually uncharted. Here we report that using *ab initio* molecular dynamics and path integral simulations based on density functional theory, a new atomic phase is discovered, which gives an uplifting melting curve of dense hydrogen when beyond 2 TPa, and results in a reentrant solid-liquid transition before entering the Wigner crystalline phase of protons. The findings greatly extend the phase diagram of dense hydrogen, and put metallic hydrogen into the group of alkali metals, with its melting curve closely resembling those of lithium and sodium.

Under compression conditions, hydrogen and alkali metals have unfolded exotic and fascinating properties, and have attracted broad attention and interests^{1–6}. Though hydrogen is assigned to the IA group in the periodic table, at low pressure it is similar to halogens rather than alkalis, with a high electronegativity and a tendency to form covalent bond with itself. At ambient conditions it exists as diatomic molecular gas, instead of in a BCC or FCC crystalline structure that usually adopted by simple metals⁷. However, recent high-pressure experiments and theoretical predictions have shed new light on their distinctions, and hinted interesting similarities and parallels for the compression behavior of dense hydrogen and light alkalis.

For example, under compression both H and Li undergo an *s-p* electronic transition, which leads to complex structure with low coordination numbers^{8–10}. In particular, Li, Na, and H all exhibit a maximum in their melting curves, as well as the subsequent *low-temperature* melting^{2–4,11}. It was speculated that except some details, the phase diagram of hydrogen and alkalis should be qualitatively similar. This paralleling, however, is questioned when going to higher pressures, where hydrogen was predicted to continuously lower its melting curve and enter an *ultra-cold* quantum liquid^{1,12,13}, whereas both experiments and theoretical calculations indicated a follow-up increase of the melting temperature for Li and Na. On the other hand, a recent deliberate calculation² suggested a flat melting curve for dense hydrogen between 500 GPa and 1.5 TPa. This variation resembles the melting minimum observed in both Li and Na^{3,4}. We will strengthen this parallelism below, by unveiling a new atomic phase of dense hydrogen and the concomitant ascent of the melting curve when beyond 2 TPa, with the melting temperature T_m reaches ~700 K at 7 TPa. This discovery greatly enhances the occurrence probability of solid metallic hydrogen in the core of *cold* giant gas planets.

The computed melting curve is drawn as the filled square-solid line in Fig. 1. We found that the T_m of H is flat between 500 to 1500 GPa, as demonstrated in ref. 2. It however increases rapidly as compression goes further and transition into a new atomic phase. This ascent is intriguing since a zero Kelvin quantum liquid of dense hydrogen had been hypothesized in this pressure range^{1,12,13}. Analysis shows that the melting minimum created by this reentrant transition, which spans from 500 GPa to 1.5 TPa, is a direct consequence of the competition between chemical covalent bonding (that favors *quasi*-molecular motifs) and pressure-induced orbital delocalization (that prefers metallization)¹⁴. The resultant frustration greatly weakens the crystalline ordering. It lowers the melting curve to a minimal level, which coincides exactly with the H₂ dissociation line, as illustrated in Fig. 1. This mechanism naturally interprets the melting maximum presented in the molecular phase of H₂ at ~100 GPa: the compression-driving evolution towards H₂ dissociation, or the gradually increased occupation of electrons in the

National Key Laboratory of Shock Wave and Detonation Physics, Institute of Fluid Physics, CAEP; P.O. Box 919-102, Mianyang, Sichuan, 621900, P. R. China. Correspondence and requests for materials should be addressed to H.Y.G. (email: s102genghy@caep.cn)

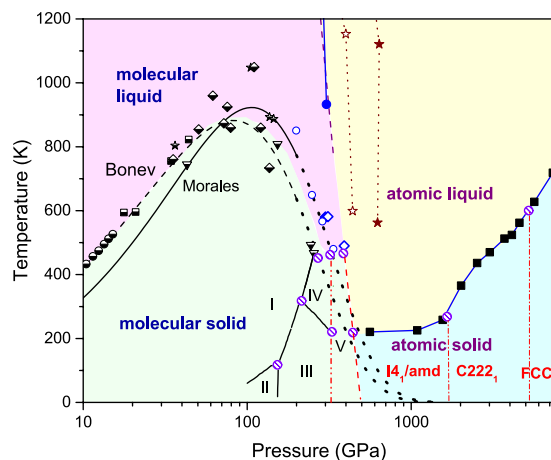


Figure 1. Phase diagram of dense hydrogen. Theoretical melting points: the filled squares above 1.5 TPa are obtained in this work, those between 500 GPa to 1.5 TPa are taken from ref. 2; rhombuses—diatomic molecular $Cmca-4$ (filled—Liu *et al.*²⁹, opened—from ref. 2), open circles—Belonoshko *et al.*²⁸, solid line—Morales *et al.*³³, dashed line—Bonev *et al.*¹⁵, and dotted lines—the extrapolation of them using Kechin's equation. Experimental data on H_2 melting: half-filled symbols (circles—Datchi *et al.*³⁴, squares—Gregoryanz *et al.*²⁷, stars—Eremets *et al.*²⁵, rhombuses—Subramanian *et al.*²⁶, triangles—Howie *et al.*¹¹). Experimental data on H_2 dissociation: blue filled circles—Knudson *et al.*²². Dashed lines are theoretical H_2 dissociation, for which the liquid part is from PIMD + vdW-DF2 data of Morales *et al.*³⁰, and the solid part is a coarse estimation by using AIMD and ground-state DFT results, and is a guide to the eye only; the star-dotted lines indicate the dissociation region estimated by VMC-MD¹⁸. Solid molecular phase boundaries (I, II, III, and IV) are from refs 11 and 35, the boundary of phase V (vertical dash-dot-dot line) is inferred from ref. 6 and is extended to low temperatures, and those of atomic solid (dash-dotted vertical lines) are guides to the eye only. Hatched circles denote possible triple points.

σ^* anti-bonds and p orbitals, weakens the crystalline stability¹⁵. Beyond this reentrant melting, Fig. 1 indicates an energy gain by crystalline ordering from the metallic interaction that prevailing at TPa regime.

Similar phenomenon has been observed in Li and Na, where the melting minimum is created mainly because of $s-p(-d)$ transition^{3,4}. There are no molecular phases involved in dense Li and Na, but strong competition between chemical bonding and metallic interaction still presents, as the tendency towards pairing and formation of low-symmetric structures with low-coordination numbers that frequently observed in dense Li and Na unequivocally illustrated^{8–10}. Analogously, the wide flat range of T_m beyond H_2 dissociation as shown in Fig. 1 is also considered as due to excitation of some electrons to orbitals with p character, as implied by the H_3 units and chain structures prevailing in many (meta-)stable solid structures predicted in this pressure range^{5,14}.

In particular, our results show that the previously proposed groundstate¹⁶ $Cmcm-8$ (a structure has the $Cmcm$ space group symmetry with 8 atoms in the primitive cell) is thermodynamically unstable with respect to a newly discovered $C222_1-8$ phase. The number of atoms in the primitive cell will not be given explicitly below for the sake of brevity. For example, $Cmcm-8$ will be abbreviated to $Cmcm$ if there is no confusion. The discovery of a new stable structure by MD simulations signals the challenge in structure prediction based solely on the static lattice enthalpy and harmonic phonons. The latter explores only a small area surrounding the ideal atomic positions, thus incapable of describing the lattice dynamics of dense hydrogen reliably¹⁴. In terms of static lattice enthalpy, the phases of $Cmcm$ and $C222_1$ are almost degenerated, as demonstrated in Fig. 2(a), in which the enthalpies are represented as a difference with respect to a predefined equation of state. The $C222_1$ structure has an enthalpy slightly lower than that of $Cmcm$. But the difference is less than 1.5 meV/H. When classical nuclear motions are included by using AIMD simulations, however, the $Cmcm$ phase spontaneously collapses into $C222_1$ phase at an equilibrated temperature as low as 20 K. This transition keeps the orthorhombic lattice unchanged but the symmetry is lowered by local atomic displacements, implying that dense hydrogen still disfavors highly symmetric structures even at such high pressures. The electron localization function (ELF) as shown in Fig. 2(a) clearly unveils that the stability of this phase closely relates to the competition between residual chemical bonding and nascent metallic interactions: the $Cmcm$ phase shows obvious H_2 bonding within the H_3 unit, whereas such pairing does not present in the $C222_1$ structure. Namely, it is the distortion away from this kind of quasi-molecular motifs that lowers the structural symmetry^{5,14,16}.

It should be pointed out that such quasi-molecular units also exist at low pressures down to 500 GPa. But in that pressure range they are meta-stable and the groundstate is the degenerated atomic phases of $I4_1/amd-2$ (which is also the Cs-IV phase) and/or $Fddd-2$ (a distortion of the Cs-IV phase)¹⁴. Strong compression increases the occupation of electrons on the anti-bonding σ^* states¹⁷, some electronic orbitals even have p character. One consequence of this effect is the creation of the melting minimum and the dissociation of hydrogen from molecular state into atomic state at around 400–500 GPa^{5,17,18}. The reappearance of quasi-molecular units in the $Cmcm$ and $C222_1$ phases at ultra-high pressure of terapascals therefore cannot be attributed to enhancement of the chemical interactions by compression. One interpretation is that compression brings protons close enough

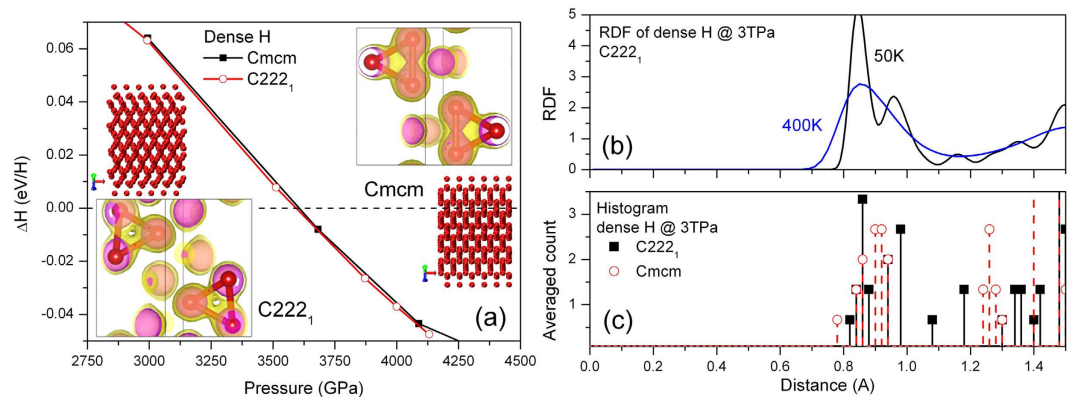


Figure 2. New candidate phase $C222_1$ in dense hydrogen. (a) Structure and electron localization function (ELF) in $Cmcm$ and $C222_1$ phases at 3 TPa, and their enthalpy difference with respect to a predefined equation of state, (b) RDF of $C222_1$ at finite temperatures, (c) inter-proton separation histogram for the static lattice of $C222_1$ and $Cmcm$ structures.

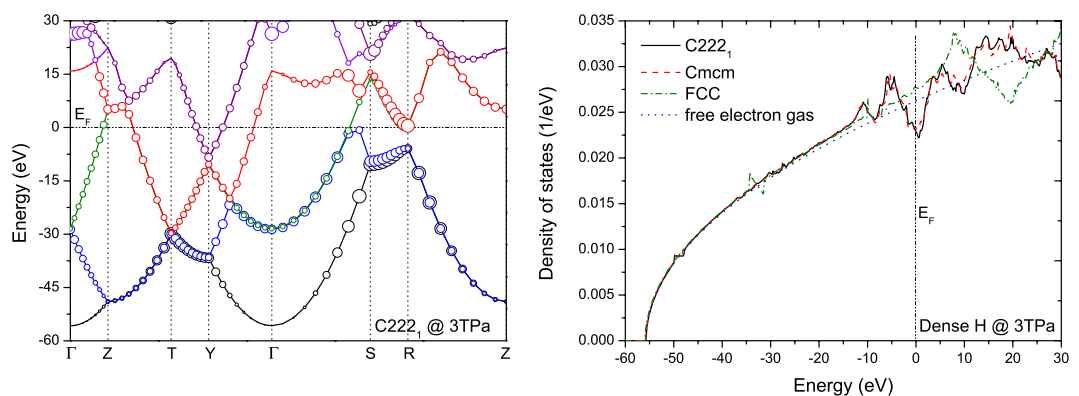


Figure 3. Nearly free electronic structure in dense hydrogen. (left) Band structure of $C222_1$ phase at 3 TPa, the size of circles is proportional to the p character of the wave functions, and (right) the density of states per electron for $C222_1$, $Cmcm$, and FCC phases of dense hydrogen at 3 TPa, and that of free electron gas, respectively.

(to $\sim 0.84 \text{ \AA}$) so that the continuously *diminishing* chemical bonding can still play its role to some extent¹⁷. We indeed find that such bonding is very weak and can be easily destroyed by nuclear thermo-motions.

The key structural feature that differentiates phase $C222_1$ from $Cmcm$ is that the former does not have a clear-cut coordination number gap as the latter at a radius between 0.94 and 1.24 \AA . Therefore, atoms in the $C222_1$ phase can access a larger configurational space than in the $Cmcm$ phase, and thus has greater entropy. The lack of a coordination gap also implies that $C222_1$ is more *metallic* than the $Cmcm$ phase. Dense hydrogen is obviously prone to this atomic structure when nuclear kinetics is taken into account, and the H_3 units might be just transient clusters, as suggested by the radial distribution function (RDF) of this structure at finite temperatures shown in the inset of Fig. 2(b). At 50 K, the first coordination shell of $C222_1$ splits into two peaks, with the first sub-shell contains 6.7 protons in average and 5.3 protons in the second one. At higher temperatures, however, these peaks merge into a single one, with 12 protons as the nearest neighbors, the same coordination number as the close-packed simple metals⁷.

The electronic structure of these phases corroborates above observations exactly. As can be seen from Fig. 3, they are very similar to the nearly free electron gas model for simple metals, which is particularly evident for the FCC structure. Both $Cmcm$ and $C222_1$ phase show similar features: In the vicinity of the Fermi level a pseudo-gap is created. This dip in the density of states could be ascribed to charge density wave, a mechanism commonly observed in alkalis⁷. Alternatively, it can approximately be interpreted as due to the formation of weak chemical bonds in real space, which is helpful for understanding the *quasi*-molecular H_3 unit. The band structure plotted in Fig. 3 shows that p orbitals take an important role in the stability of these phases. All of the states near the Fermi level show pronounced p character, and it is the splitting of the states along the S - R direction in the reciprocal space that opens the pseudo-gap up, as a result of strong hybridization between s and p orbitals. In other words, it is the compression that brings nearest-neighboring hydrogen atoms to a distance close enough and the subsequent sp hybridization that stabilizes $C222_1$ and $Cmcm$ phases.

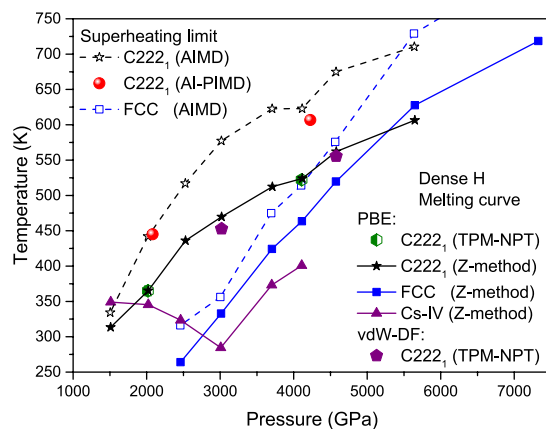


Figure 4. Uprising of the melting temperature in dense hydrogen. The calculated melting curves (for the $C222_1$, FCC, and Cs-IV phases, respectively) and superheating limit (only for the $C222_1$ and FCC phases) of dense hydrogen from 1.5 to 7.3 TPa in several candidate solid phases by different *ab initio* simulation methods, which indicates the progressive enhancement of the stability of the solid phases of atomic hydrogen by compression. The previously speculated melting temperature is far lower and approaching 0 K.

Though $Cmcm$ and $C222_1$ have similar electronic structure at the static lattice approximation, different from $Cmcm$, the dynamical stability of $C222_1$ structure is quite robust. It possesses the highest melting temperature and the highest superheating limit from 2 to 5 TPa among all studied structures (Fig. 4). The $cI16$ phase has the second highest melting curve (not shown). Beyond 5.3 TPa the high-symmetric FCC becomes the most stable solid phase with the highest melting temperature and the highest superheating limit, followed by BCC as the second stable one. It is interesting to observe that $I4_1/amd$ phase reaches a melting minimum at about 3 TPa (where it becomes metastable), suggesting that the stabilization of this phase at lower pressures^{5,14} is actually resultant from interaction frustration. It also should be noted that at around 4 TPa, the FCC phase can be stabilized by a pure exponentially decayed repulsive potential, demonstrating that the dense hydrogen already entering the Wigner crystal region¹⁹.

Because the Z-method is prone to overestimating the T_m in some systems², in order to verify its validity, we also calculate T_m by using the two-phase method with NPT ensemble (TPM-NPT)²⁰. At 2 and 4 TPa, the obtained T_m by TPM-NPT method perfectly overlap with the results of Z-method (Fig. 4), justifying that Z-method works well in dense hydrogen². The application of PBE functional to metallic hydrogen with quasi-molecular units might also raise some concerns, since it is well-known that H_2 dissociation is poorly described by this functional. Nonetheless, considering the nearly free electronic features as revealed in Fig. 3, it is plausible to expect that PBE performs well in this circumstance. This argument is justified by using the van der Waals functional vdW-DF with TPM-NPT method, as shown in Fig. 4. This van der Waals functional has been carefully examined recently and was shown of good performance in H_2 dissociation by comparison to both accurate QMC simulation²¹ and dynamic compression experiment²². The good agreement of the T_m calculated by vdW-DF and PBE functionals unequivocally demonstrates the validity of PBE approximation at such high pressures. The NQE on the phase stability and superheating limit is assessed by using *ab initio* path integral MD (AI-PIMD)^{2,19}. The conclusion is that the NQE correction is very small, as demonstrated by the superheating limit T_{sl} of the $C222_1$ phase in Fig. 4. This is drastically different from the $Fddd$ and Cs-IV phases at pressures between 500 and 1500 GPa, where a pronounced NQE was observed^{1,2}. It is worth mentioning that this does not imply that the absolute contribution of NQE to the free energy is small. Rather, it simply indicates a cancellation of the NQE contribution between the liquid and solid phases. Similar cancellation was also observed in the melting of Li²³. These observations consolidate and validate the melting curve obtained with Z-method.

One of the main findings is that beyond 3 TPa, all considered candidate solid phases enhance their stability with increasing pressure, which is reflected in the ascending T_m and T_{sl} . Our work reveals that this increase of the stability is dominated by the potential energy surface. NQE has little influence on this respect. This discovery might be helpful for searching for the quantum liquid of metallic hydrogen, which was speculated as a superconducting superfluid²⁴ at a pressure range of 0.5–1.5 TPa, where a metastable supercooled liquid state might exist². When beyond 7 TPa, our result indicates that nuclear-nuclear repulsion takes the main role in determining the atomic structure, and the electronic structure can be described by a free electron gas model. Therefore, low-symmetric structures such as those presented between 0.2 to 5 TPa are unlikely any more. On the other hand, theoretical analysis suggested that in Wigner crystalline phases, the BCC is slightly stable than FCC phase, thus there might still have a FCC \rightarrow BCC transition at higher pressures. Beyond that there would have no other solid-solid phase transition can be expected, except the nontrivial melting of Wigner crystals induced by enormous nuclear quantum kinetic energy.

The finally obtained phase diagram is summarized and plotted in Fig. 1, in which the vertical dash-dotted lines that separate atomic solid phases are roughly based on the intersections of the respective melting curves, and are guides to the eye only. Reliable experimental data about the melting of dense hydrogen^{11,25–27} available so far are also included for comparison (here we do not distinguish the data made on deuterium from those on hydrogen,

since at high temperatures the isotopic effect is small and they become similar). Especially, the recent Raman data, which did not measure the molecular solid phase melting directly but gave a hint about the lower bound of the melting curve, suggested that the melting temperature of dense molecular hydrogen indeed decreases with increasing pressure, and follows the variation trend predicted by the Kechin's equation up to 250 GPa¹¹. These experimental data are in good agreement with the theoretical predictions given in refs 2, 28 and 29. This, from another point of view, is a direct experimental validation of the theoretical method we employed. A triple point between phases I-IV-liquid was also hinted in the Raman spectroscopy experiment¹¹. It implied that the slope of the melting curve could increase slightly beyond that triple point. The theoretical data of the melting curve around this pressure do hint such a slight change. This comparison also implies other two triple points between phases IV, V, and the molecular liquid, and that between phase V, the molecular liquid, and the atomic liquid. It is worth pointing out that both the dissociation line predicted by ref. 30 and the recent dynamic experimental data by ref. 22 match very well with each other, and all point to the coalescence with the melting curve at about 490 K and 390 GPa. This dissociation line separates the semiconducting and metallic states in the liquid phase, and might extend to the solid regime to separate the phase V and the atomic $I4_1/amd$ phase⁶, as the dashed line in Fig. 1 indicated.

This diagram outlines the overall structure of the phase diagram of dense hydrogen within the pressure range that will be accessible by dynamical compression in the near future³¹. It greatly advances the understanding about dense hydrogen, and unambiguously demonstrates that the cold melting of dense hydrogen directly relates to the dissociation of H₂. Namely, it is resultant from the flat potential energy surface due to the occupation of electrons on both the bonding and anti-bonding states, which leads to a strong competition and frustration between electron localization and delocalization. In addition, most gas planets contain hydrogen as the main composition with the core pressure up to terapascal scale. The findings reported here pave the way to evaluate the high-pressure properties of hydrogen-rich minerals and rocks that are crucial for modelling the interior structure and dynamical evolution of these planets. The computation and analysis techniques employed here could also be applied to assess the phase diagram of other substances under extreme conditions.

Methods

Electronic structure calculations. The density functional theory is used to describe the electronic structures. The interaction between electrons and protons is described by all-electron projector augmented wave (PAW) method, and the Perdew-Burke-Ernzerhof (PBE) electronic exchange-correlation functional is employed. Both the standard and the hard version of the PAW pseudopotentials provided in VASP code are used. The validity of these potentials is carefully checked against the all-electron full-potential results of WIEN2k, as prescribed in ref. 2. An energy cutoff of 700 eV is used for the plane-wave expansion of the valence and conduction band wave functions. A $3 \times 3 \times 3$ Monkhorst-Pack k -point mesh is used to sample the first Brillouin zone. A larger $4 \times 4 \times 4$ mesh is also used to check the convergence quality. The size of the simulation cell varies from containing 432 to 500 hydrogen atoms depending on the candidate solid structures, with periodic boundary conditions being imposed.

Melting curve calculations. The melting curve of dense hydrogen is modeled using *ab initio* molecular dynamics (AIMD) simulations. In order to obtain a reliable melting curve, the ground-state candidate structures that are predicted to be stable at this ultra-high pressure range and all other known low-lying structures are explored, including the $Fddd$ and Cs-IV phases¹⁴, hexagonal and planar $R\bar{3}m$, triatomic $R3m$ and $Cmcm$ phases, the high-symmetric BCC and FCC, and cI16- $I\bar{4}3d$ phases⁵, etc. The cI16 is a distortion of the BCC structure and is also the high-pressure phase reported for Li and Na when the slope of their melting curve becomes positive again⁹. It is necessary to point out that it is impossible to consider all possible structures. The physical melting temperature always corresponds to that of the structure that has the highest T_m , and what we obtained here is an estimate of the lower bound of the melting curve. The true T_m might be higher if structures more stable than we employed here were found. However, this will not modify our conclusion that the melting curve of metallic hydrogen has a positive slope when beyond 2 TPa. The Z-method that is widely used to model homogeneous melting is employed³². In order to check whether this method overestimates T_m or not, two-phase method calculations in NPT ensemble are also performed. In these simulations, the van der Waals functional vdW-DF is also used to justify the performance of PBE functional for dense atomic hydrogen. The facts of the perfect agreement of the T_m predicted by these two functionals, and the good performance of van der Waals functional in describing H₂ dissociation by comparison with QMC²¹ and dynamic compression experiment²², give a strong support to the reliability of our DFT results. In fact, the validity of PBE functional in metallic hydrogen had been verified by method beyond DFT, such as the coupled electron-ion Monte Carlo simulations (CEIMC)³³. The timestep of AIMD simulation is set as 0.5 fs. All simulated systems were observed to equilibrate rapidly within 0.5 ps. Moreover, all AIMD simulations run for at least 4 ps to collect enough data for statistics analysis. Other details of the simulations are given in the supplementary information.

Nuclear quantum effects. NQE influence is modelled using path integral AIMD simulations, in which a homemade code¹⁹ is used. Due to the possible ambiguity of two-phase method in NVT ensemble², and considering the fact that there are no path integral algorithms for two-phase method in NPT or Z -method in NVE ensemble available currently, we did not calculate the NQE on melting directly, but turned to compute the NQE on superheating limit using a *heat-until-melting* approach. Since both T_m and the superheating limit are at the same temperature level, the NQE corrections on them should be similar. The careful two-phase calculations as reported in ref. 2 lend us the confidence of the validity of this treatment in dense hydrogen. Considering that the relevant temperature scale studied in this work is high enough, we employed 8 beads to discretize the integral path. The convergence quality is checked by using 32 beads, which do not change the results substantially.

References

- Chen, J. *et al.* Quantum simulation of low-temperature metallic liquid hydrogen. *Nat. Commun.* **4**, 2064 (2013).
- Geng, H. Y., Hoffmann, R. & Wu, Q. Lattice stability and high-pressure melting mechanism of dense hydrogen up to 1.5 TPa. *Phys. Rev. B* **92**, 104103 (2015).
- Guillaume, C. L. *et al.* Cold melting and solid structures of dense lithium. *Nat. Phys.* **7**, 211 (2011).
- Gregoryanz, E., Degtyareva, O., Somayazulu, M., Hemley, R. J. & Mao, H. K. Melting of dense sodium. *Phys. Rev. Lett.* **94**, 185502 (2005).
- McMahon, J. M., Morales, M. A., Pierleoni, C. & Ceperley, D. M. The properties of hydrogen and helium under extreme conditions. *Rev. Mod. Phys.* **84**, 1607 (2012).
- Dalladay-Simpson, P., Howie, R. T. & Gregoryanz, E. Evidence for a new phase of dense hydrogen above 325 gigapascals, *Nature* **529**, 63 (2016).
- McMahon, M. I. & Nelmel, R. J. High-pressure structures and phase transformations in elemental metals. *Chem. Soc. Rev.* **35**, 943 (2006).
- Naumov, I. I. & Hemley, R. J. Origin of transitions between metallic and insulating states in simple metals. *Phys. Rev. Lett.* **114**, 156403 (2015).
- Rousseau, B., Xie, Y., Ma, Y. & Bergara, A. Exotic high pressure behavior of light alkali metals, lithium and sodium. *Eur. Phys. J. B* **81**, 1 (2011).
- Naumov, I. I., Hemley, R. J., Hoffmann, R. & Ashcroft, N. W. Chemical bonding in hydrogen and lithium under pressure. *J. Chem. Phys.* **143**, 064702 (2015).
- Howie, R. T., Dalladay-Simpson, P. & Gregoryanz, E. Raman spectroscopy of hot hydrogen above 200 GPa. *Nature Mater.* **14**, 495 (2015).
- Ashcroft, N. W. The hydrogen liquids. *J. Phys.: Condens. Matter* **12**, A129 (2000).
- Kechin, V. V. Melting of metallic hydrogen at high pressures. *JETP Lett.* **79**, 40 (2004).
- Geng, H. Y., Song, H. X., Li, J. F. & Wu, Q. High-pressure behavior of dense hydrogen up to 3.5 TPa from density functional theory calculations. *J. Appl. Phys.* **111**, 063510 (2012).
- Bonev, S. A., Schwegler, E., Ogitsu, T. & Galli, G. A quantum fluid of metallic hydrogen suggested by first-principles calculations. *Nature* **431**, 669 (2004).
- Liu, H., Wang, H. & Ma, Y. Quasi-molecular and atomic phases of dense solid hydrogen. *J. Phys. Chem. C* **116**, 9221 (2012).
- Labet, V., Hoffmann, R. & Ashcroft, N. W. A fresh look at dense hydrogen under pressure. III. Two competing effects and the resulting intra-molecular H-H separation in solid hydrogen under pressure. *J. Chem. Phys.* **136**, 074503 (2012). A fresh look at dense hydrogen under pressure. IV. Two structural models on the road from paired to monatomic hydrogen, via a possible non-crystalline phase. *J. Chem. Phys.* **136**, 074504 (2012).
- Mazzola, G. & Sorella, S. Distinct metallization and atomization transitions in dense liquid hydrogen. *Phys. Rev. Lett.* **114**, 105701 (2015).
- Geng, H. Y. Accelerating *ab initio* path integral molecular dynamics with multilevel sampling of potential surface. *J. Comput. Phys.* **283**, 299 (2015).
- Belonoshko, A. B. Molecular dynamics of MgSiO₃ perovskite at high pressures: Equation of state, structure, and melting transition. *Geochim. et Cosmochim. Acta* **58**, 4039 (1994).
- McMinis, J., Clay III, R. C., Lee, D. & Morales, M. A. Molecular to atomic phase transition in hydrogen under high pressure. *Phys. Rev. Lett.* **114**, 105305 (2015).
- Knudson, M. D. *et al.* Direct observation of an abrupt insulator-to-metal transition in dense liquid deuterium. *Science* **348**, 1455 (2015).
- Feng, Y. *et al.* Nuclear quantum effects on the high pressure melting of dense lithium. *J. Chem. Phys.* **142**, 064506 (2015).
- Babaev, E., Sudbø, A. & Ashcroft, N. W. A superconductor to superfluid phase transition in liquid metallic hydrogen. *Nature* **431**, 666 (2004).
- Eremets, M. I. & Trojan, I. A. Evidence of maximum in the melting curve of hydrogen at megabar pressures. *JETP Lett.* **89**, 174 (2009).
- Subramanian, N., Goncharov, A. F., Struzhkin, V. V., Somayazulu, M. & Hemley, R. J. Bonding changes in hot fluid hydrogen at megabar pressures. *Proc. Natl. Acad. Sci. USA* **108**, 6014 (2011).
- Gregoryanz, E., Goncharov, A., Matsuishi, K., Mao, H.-K. & Hemley, R. Raman spectroscopy of hot dense hydrogen. *Phys. Rev. Lett.* **90**, 175701 (2003).
- Belonoshko, A. B., Ramzan, M., Mao, H. K. & Ahuja, R. Atomic diffusion in solid molecular hydrogen. *Sci. Rep.* **3**, 2340 (2013).
- Liu, H., Zhu, L., Cui, W. & Ma, Y. Room-temperature structures of solid hydrogen at high pressures. *J. Chem. Phys.* **137**, 074501 (2012).
- Morales, M. A., McMahon, J. M., Pierleoni, C. & Ceperley, D. M. Nuclear quantum effects and nonlocal exchange-correlation functionals applied to liquid hydrogen at high pressure. *Phys. Rev. Lett.* **110**, 065702 (2013).
- Smith, R. F. *et al.* Ramp compression of diamond to five terapascals. *Nature* **511**, 330 (2014).
- Belonoshko, A. B., Skorodumova, N. V., Rosengren, A. & Johansson, B. Melting and critical superheating. *Phys. Rev. B* **73**, 012201 (2006).
- Morales, M. A., Pierleoni, C., Schwegler, E. & Ceperley, D. M. Evidence for a first-order liquid-liquid transition in high-pressure hydrogen from *ab initio* simulations. *Proc. Natl. Acad. Sci. USA* **107**, 12799 (2010).
- Datchi, F., Loubeyre, P. & LeToullec, R. Extended and accurate determination of the melting curves of argon, helium, ice (H₂O) and hydrogen (H₂). *Phys. Rev. B* **61**, 6535 (2000).
- Howie, R. T., Guillaume, C. L., Scheler, T., Goncharov, A. F. & Gregoryanz, E. Mixed molecular and atomic phase of dense hydrogen. *Phys. Rev. Lett.* **108**, 125501 (2012).

Acknowledgements

This work was supported by the National Natural Science Foundation of China under Grant Nos 11274281 and 11672274, and by the CAEP Research Projects under Grant No. 2012A0101001 and No. 2015B0101005. Part of computation was performed on CCMS of the Institute for Materials Research at Tohoku University, Japan.

Author Contributions

H.Y.G. conceived the project and performed the calculations. H.Y.G. and Q.W. analyzed the data and wrote the manuscript.

Additional Information

Supplementary information accompanies this paper at <http://www.nature.com/srep>

Competing financial interests: The authors declare no competing financial interests.

How to cite this article: Geng, H. Y. and Wu, Q. Predicted reentrant melting of dense hydrogen at ultra-high pressures. *Sci. Rep.* **6**, 36745; doi: 10.1038/srep36745 (2016).

Publisher's note: Springer Nature remains neutral with regard to jurisdictional claims in published maps and institutional affiliations.



This work is licensed under a Creative Commons Attribution 4.0 International License. The images or other third party material in this article are included in the article's Creative Commons license, unless indicated otherwise in the credit line; if the material is not included under the Creative Commons license, users will need to obtain permission from the license holder to reproduce the material. To view a copy of this license, visit <http://creativecommons.org/licenses/by/4.0/>

© The Author(s) 2016